Radioisotope Power Source Dose Estimation Tool (RPS-DET)

Michael B. R. Smith
Oak Ridge National Laboratory
1 Bethel Valley Road, P.O. Box 2008, Oak Ridge, TN, 37931
865-314-9717, smithmb@ornl.gov

Abstract—**The purpose of this work is to develop a radioisotope power source dose estimation tool (RPS-DET) capable of rapidly predicting accurate neutron and gamma-ray flux/dose implications from various radioisotope power sources (RPSs). RPS-DET can use this information to calculate the flux/dose incident on or absorbed by nearby humans, materials, and electronics over a complex mission lifetime. This simulation tool uses a Matlab user interface to combine common geometry scenarios for traditional and new RPS design configurations to write a particle-transport simulation using Monte Carlo N-Particle (MCNP) 6, which provides results that are automatically post-processed for interactive analysis. The user defines the average age of the PuO_2 fuel, which determines the appropriate time-dependent gamma-ray and neutron spectra, along with the desired RPS and local environment for the simulation. Results for a given simulation are gamma-ray, neutron, and combined flux spectra, whole-body effective dose for humans, and absorbed dose in silicon for electronics. This work has been benchmarked against measurements of existing RPS units and has been determined to predict neutron and gamma flux, absorbed dose, and dose equivalent within 50% of simulation uncertainties.**

TABLE OF CONTENTS

1. INTRODUCTION

Radioisotope power sources (RPSs) have been used for over 50 years to supply electrical power to spacecraft and planetary rovers by converting thermal decay heat of radioactive materials into electrical power [1]. Although various permutations of RPSs have been investigated and used, a resurgence of interest in dynamic RPS (DRPS) systems has prompted a call from the National Aeronautics and Space Agency (NASA) to industry to propose new dynamic conversion technologies [2]. The proposed technologies are individually evaluated for technology claims, performance concerns, material implications, and spacecraft integration. As part of this investigation, radiation created by the DRPS fuel (PuO_2) must be estimated to fully understand dose implications to surrounding people, electronics, and other materials of concern. The RPS Dose Estimation Tool (RPS-DET) was developed to rapidly and accurately perform this task while focusing on three core innovations in rapid simulation abilities: combinations of simulations based on providing multiple RPS fuel-configurations (static and dynamic) and RPS designs, multiple surrounding environments, and the ability to have time-dependent neutron and gamma-ray source terms (i.e., "aging" the fuel).

978-1-5386-2014-4/18/$31.00 ©2018 IEEE

Importance of Representing Different RPS Units

Understanding and predicting the full implications of radiation effects caused by RPS fuel configuration and system design are crucial for understanding the biological dose consequences for workers as new more complex designs may come into favor. These new designs may have new radiation implications requiring new procedural methods during assembly and installation. This could result in new occupational exposure times that will factor into an evaluation of any given new RPS system being investigated. Neutron and gamma fields emitted from the fuel affect electronics and avionics systems, causing a rise in the probability of adverse electronic effects such as bit-flips or single event upsets (SEUs). Over time, these factors can cause malfunctions in avionics systems [3]. Being able to predict the probability of electronic failure over a given mission lifetime for a specific RPS will help guide engineers in identifying optimal locations for electronics distributed around the fuel. Finally, as new dynamic designs are proposed and evaluated, radiation effects on materials not traditionally found in radioisotope thermoelectric generator (RTG) technologies such as bearings, gaskets, low-friction coatings, working fluids, etc., need to be evaluated to aid in estimating any potential for concern from material irradiation.

Importance of Representing Different Environments

Although a given RPS system will produce a mixed radiation field based on fuel amount, fuel configuration, and convertor materials, the ambient environment of the unit can also greatly alter the external and internal radiation field. When analyzing the radiation effects of a given RPS, one must consider that this single unit will be subject to multiple environments throughout its life, and each environment will have a different effect on an ambient radiation field. For example, the Mars Science Laboratory (MSL) power source is an RPS design called the *multi-mission RTG* (MMRTG). This RPS model requires a known amount of exposure time for occupational workers during fabrication, assembly, transportation, and spacecraft integration. During this period of the MMRTG's life, it was surrounded by atmospheric air, transported in shipping casks, placed on truck beds, sitting on concrete floors, and suspended by cranes while being in regular contact with occupational workers, resulting in varying biological dose concerns. For launch, the MMRTG was integrated into the MSL module, where it was adjacent to many electrical components in the transport capsule and on the MSL Rover. After the launch vehicle left Earth's atmosphere, the environment of the MMRTG was in the same physical configuration for the duration of the transit to Mars, but it was now in the vacuum of space, which alters the radiation signature and affects the dose implications to the surrounding electronics. Upon landing on Mars, the MMRTG was surrounded by the Martian atmosphere (~98% CO_2) outside the transit capsule, suspended ~80cm above the Martian regolith while attached to the aft portion of the MSL Rover (Curiosity Rover) [4] (Figure 1 [5]).

This is one of many potential examples illustrating how each RPS can anticipate occupying several environments throughout a mission-lifetime, and it demonstrates the importance of having a flexible tool that allows rapid simulation of multiple RPS models in varying environments to provide a more accurate estimate of integrated fluxes/doses over a complex mission lifetime. The RPS-DET terminology for individual environments is *environments of interest* (EOIs).

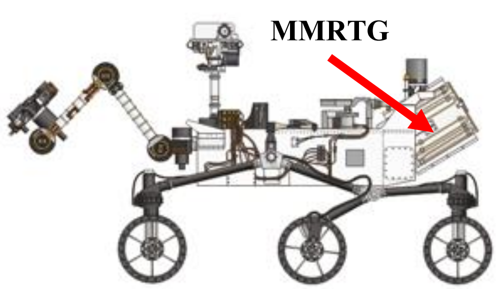

Figure 1. Mars Curiosity Rover showing MMRTG configuration

Importance of Representing Time-Dependent Fuel

To perform accurate integrated dose/flux calculations, one must also account for the fuel's activity and energy-dependent flux spectra changing over time (see Section 2, "Tallies"). For PuO_2 fuel, the neutron spectrum comes from spontaneous fission and (α, n) reactions on low-Z elements [6]. Although the energies of the neutron spectra will not significantly shift over the life of the fuel, the overall activity will consistently decrease by approximately 1.0% per year (Section 2, "Time-Dependent Gamma-Ray Spectra"). Conversely, the high-energy gamma-ray activity will increase by nearly an order of magnitude in the first 15 years, and discrete energies of the spectra will appear as plutonium isotopes decay into radioactive daughter products that emit unique and highly energetic spectra (Section 2, "Time-Dependent Neutron Spectra"). To provide accurate integrated dose estimates over long periods of time for RPS units using PuO_2 fuel, a single value for the fuel's activity and spectra is not sufficient, and time-dependent aspects of fuel aging must be addressed.

2. Radioisotope Power Source Dose Estimation tool (RPS-DET)

This paper outlines the development and use of a new RPS-DET for estimating dose implications of various dynamic and static RPS systems in various environments relevant to terrestrial fabrication, unmanned space/planetary scenarios, and manned space/planetary scenarios for RPS systems using GPHSs.

RPS-DET uses Matlab as a user interface to develop the input files for Monte-Carlo (MC) simulations based on the combination of specific RPS designs and configurations in various surrounding environments. These input files are used to execute the simulation and calculate the flux, absorbed dose, effective dose, and dose-equivalent results. Unless specifically defined, the terms *biological effective dose*, *dose equivalent*, *absorbed dose*, and *absorbed dose in silicon* are collectively referred to as *dose* from this point forward.

The input files compiled by RPS-DET are used by MCNP6, a well-established MC code for particle transport developed at Los Alamos National Laboratory (LANL) [7]. Each MCNP6 simulation is defined by an input file, or input deck, with information about the simulation's geometry, materials, source definition, and particle tallies.

Typically, a single input deck is written for an individual MCNP6 simulation, and the modeler includes all the specific information required to accurately perform the analysis in a single unchanging file. RPS-DET adds flexibility in the creation of input decks by using a pre-established library of input deck information that can be selected and combined depending on the user's desired simulation scenario. RPS-

DET is structured to automatically combine various objects of interest (OOIs) with various EOIs within the final geometry, and it provides the ability to combine a specific photon and neutron source, depending on the age of fuel the user wishes to simulate. For example, the photon source term of PuO_2 changes significantly over the first ~20 years of its life. The ability to combine any selection of the currently available 29 OOIs, 17 EOIs, and 100 years of fuel age yields a large simulation-space of possible geometries without requiring that every possible combination be explicitly written (Figure 2).

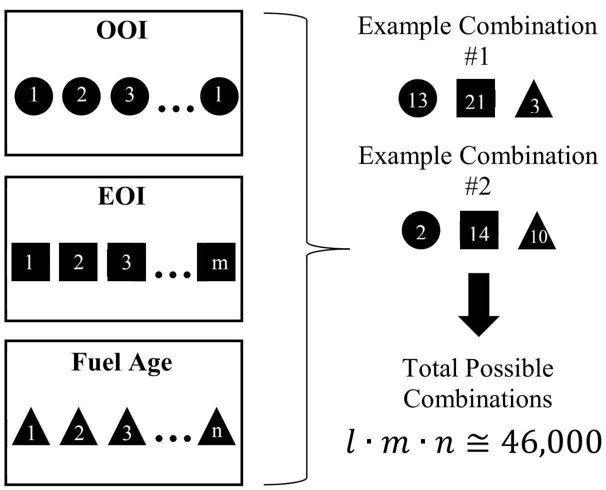

Figure 2. Illustration of possible combinations of OOIs and EOIs evaluated at different fuel ages.

Each simulation's results are processed in three-dimensional flux/dose plots, two-dimensional flux/dose contour maps, two-dimensional flux/dose centerline plots, and integrated biological dose as a function of average proximity to the RPS, fuel age, and mission duration.

Objects of Interest

Objects of interest (OOIs) are defined within RPS-DET as the source of radiation, along with the associated geometry and materials in the immediate surroundings. For example, a user may choose from 29 separate OOIs to simulate within RPS-DET, and each OOI is designed to be encased in a common OOI *boundary,* an all-encompassing, commonly numbered shape that separates the OOI from the EOI. A list of all currently available OOIs is provided in Table 1.

Table 1. Available OOIs in RPS-DET Library

OOI #	OOI Brief Description
1–4	1-4 iridium-clad PuO_2 pellet (No GPHS)
5–22	1-18 GPHS module (4 PuO_2 pellets)
23	1 MMRTG (8 GPHSs) *
24	1 GPHS-RTG (18 GPHSs) *
25	1 Advanced Stirling Radioisotope Generator (ASRG, 2 GPHSs)
26–29	4 Separate Dynamic RPS Models†

* General purpose heat sources (GPHS) are vertically stacked.
† Models are not described in detail for proprietary reasons.

For all RPS-DET simulations, each iridium-clad PuO_2 fuel source or pellet has a mass of ~150 grams, and 88.2% ^{238}Pu enrichment scheme. The mass and isotopic composition is based on the average of the three RTGs used in the 1997 Cassini mission with ^{18}O impurities assumed at 20 g/µg of total oxide content (Table 2**)** [8].

Table 2. PuO_2 Material Composition

Element	% Weight PuO_2
Oxygen	11.8
Plutonium	88.2
Oxygen Isotope	**% Weight of Oxygen**
^{16}O	~9.99E-1
^{18}O	2.00E-5
Plutonium Isotope	**% Weight of Plutonium**
^{242}Pu	1.36E-3
^{241}Pu	2.18E-3
^{240}Pu	2.18E-2
^{239}Pu	1.53E-1
^{238}Pu	8.22E-1
^{236}Pu	1.18E-8

These fuel pellets serve as the central definition for the source in all RPS-DET simulations, where each pellet is identical in material composition and radiation emission characteristics, while the only difference between each permutation of the source is the number of fuel pellets and their orientation in the geometry. A photograph of a clad pellet alongside the RPS-DET's MCNP6 geometry can be seen in Figure 3 [9].

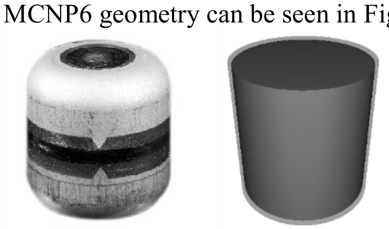

Figure 3. Photograph of real iridium-clad pellet (left) and the MCNP6 model of the pellet inside the OOI boundary (right)—images not to scale.

As mentioned above, every OOI in the RPS-DET library currently uses some arrangement and combination of these individual fuel pellets. For instance, the next step in complexity for OOIs is the incorporation of a full general purpose heat source (GPHS) module which consists of four fuel pellets placed inside a series of carbon casings (Figure 4 [10]).

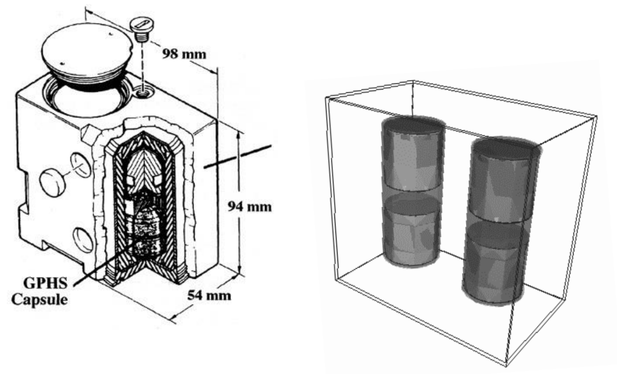

Figure 4. Schematic of a single GPHS (left) and the MCNP6 model of a GPHS (right)—images not to scale.

The GPHSs are designed to be modular so that they can be stacked together to scale up the thermal output for a given RPS system's power requirements. RPS-DET allows the user to select from one to eighteen vertically stacked GPHSs as the OOIs, but it also includes more sophisticated geometries representing common RPS systems based on the GPHS as a heat source. While all OOIs are not discussed in detail, a single, more complex example of the fuel pellets, multiple GPHSs, and additional materials are described as they would be found in a full RPS system.

One example of a complex OOI available in RPS-DET is the MMRTG. The MMRTG (Figure 5) is an RPS system used as the main power source for the MSL mission and likely the impending Mars 2020 mission [1]. It consists of eight GPHSs stacked inside layers of various insulation, shielding, and thermal conduction materials. These materials include a Haynes 25 thermal conductor, a Microtherm Super-G insulator, a Min-K insulator, and various aluminum alloys [12,13]. Because of the MMRTG's robust nature and its anticipated continued use in the space industry, it is used here as an example of a complex RPS technology available in the RPS-DET library [1].

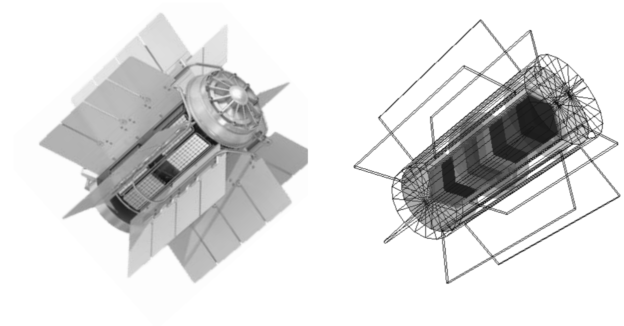

Figure 5. Image of an MMRTG (left) and the MCNP6 model of an MMRTG (right)—not to scale.

The RPS-DET imports a given OOI by reading a large text file or library with unique numerical markers surrounding each body of text defining each specific OOI. When RPS-DET chooses to include a specific OOI, it scans the library, locates the numerical marker, and imports all text, line by line, until it reaches the second closing marker. This modular design was developed to allow for simple updating of the available OOI library as new designs are chosen to evaluate.

Environment of Interest (EOI)

The available EOIs in the current RPS-DET library are based on typical scenarios for RPS units and some speculative scenarios that consider the potential for future manned missions using RPS technology and unmanned exploration of planets, moons, or asteroids. These scenarios can be seen in Table 3.

Table 3. Available EOIs for RPS-DET

EOI#	EOI Brief Description
1	Floating in a Vacuum
2	Floating in Air
3	On Steel Table, in Concrete Room, in Air
4	On Concrete Floor, in Concrete Room, in Air
5	In Hot-Cell, on Concrete Floor
6	In RPS Shipping Cask (#9904)
7	In Space Capsule, in Air
8	In Space Capsule, in Vacuum
9	On Lunar Regolith, in Vacuum
10	Buried in Lunar Regolith
11	On Martian Regolith, in Martian Atmosphere
12	Buried in Martian Regolith
13	Submerged in Freshwater
14	Submerged in Saltwater
15	In Atmosphere of Titan
16	On Ice Slab in Vacuum

Although the current EOI library is limited to 17 environmental scenarios, as geometries become more detailed and accurate for relevant environments, they will be easily incorporated into the existing library. One example of a geometry found in the RPS-DET library is the #9904 RPS shipping container [13], which is approved by the US Department of Energy (DOE), the US Nuclear Regulatory Commission (NRC), and the US Department of Transportation (DOT). The #9904 RPS shipping container is designed specifically for transportation of RPS systems from a final assembly point at Idaho National Laboratory (INL) to Cape Canaveral for launch (Figure 6) [1].

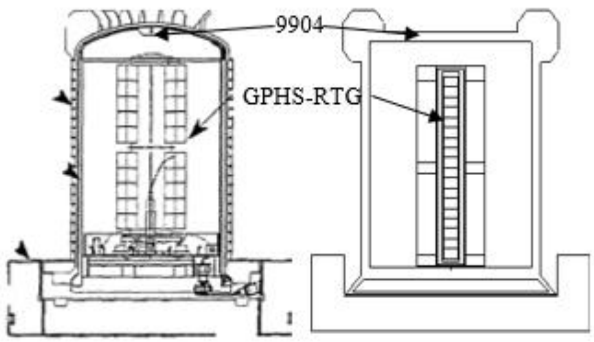

Figure 6. Schematic of #9904 shipping container containing a GPHS-RTG (left) and the MCNP6 model equivalent (right)—images not to scale.

Although the previous example shows a single OOI (the GPHS-RTG) placed inside an EOI (the shipping container), this same OOI could have been placed in any available EOI in the current RPS-DET library outlined in Table 3.

Source Particles

Fuels used in RPS technology produce a significant alpha, beta, neutron, and photon signature. Although the entire source spectrum represents a variety of particle species, the neutrons and photons above certain energies are the only types of radiation that typically penetrate the casing of the fuel-clads, GPHSs, and external RPS materials. Because external, biological, and avionics dose implications are the primary purpose for RPS-DET, all simulations are limited to the transport of neutrons and photons. The source term is defined within MCNP6 as a volumetric, isotropic distribution throughout the material previously defined in Table 2 which fully occupies the volume inside the iridium cladding in all simulated fueled-clads.

Time-Dependent Gamma-Ray Spectra

The source definition of gammas-rays, or gammas, is time dependent, and it changes with fuel age as the parent fuel decays and transmutes through its various decay chains. Because of this phenomenon, to receive an accurate estimate of the dose at a time in the life of the fuel, the user must select the age of the fuel for a given simulation, and RPS-DET will automatically define the appropriate composite gamma spectrum for the desired time frame. This method is achieved by taking the known starting composition of a PuO_2 fuel (Table 2) and the known decay channels of the plutonium parent isotopes (only ^{236}Pu and ^{238}Pu). The parent and descendant isotopes simulated by RPS-DET are outlined in Table 4.

Table 4. Simulated isotopes with half-lives for gamma source definitions in RPS-DET.

Isotope	Half Life
$^{234}U^{*}$	2.45×10^{5} (y)
$^{232}U^{\dagger}$	68.90 (y)
$^{232}Th^{\dagger}$	1.40×10^{10} (y)
$^{230}Th^{*}$	7.54×10^{4} (y)
$^{228}Th^{\dagger}$	1.91 (y)
$^{226}Ra^{*}$	1.60×10^{3} (y)
$^{224}Ra^{\dagger}$	3.63 (d)
$^{222}Rn^{*}$	3.82 (d)
$^{220}Rn^{\dagger}$	55.60 (s)
$^{212}Po^{\dagger}$	0.29 (μs)
$^{214}Bi^{*}$	19.94 (m)
$^{212}Bi^{\dagger}$	60.55 (m)
$^{210}Bi^{*}$	5.01 (d)
$^{214}Pb^{*}$	26.80 (m)
$^{212}Pb^{\dagger}$	10.64 (h)
$^{210}Pb^{*}$	22.20 (y)
$^{210}Tl^{*}$	1.30 (m)
$^{208}Tl^{\dagger}$	3.05 (m)

† ^{236}Pu decay products
* ^{238}Pu decay products

Not all isotopes in the natural decay chain are included in these simulations. Isotope inclusion was based on two criteria: (1) the isotope having ***any*** gamma energies > 30 keV, and (2) the isotope having ***any*** gamma intensities > 0.1%. If neither of these criteria was met, the isotope was not incorporated in the source term. These criteria were imposed to maximize the sampling of relevant particles at energies and intensities that significantly affect external radiation fields as opposed to sampling and simulating thousands to millions of particles that may never escape the RPS fuel, cladding, or surrounding materials.

An activation and decay program developed at Oak Ridge National Laboratory (ORNL) called IsoChain was used to solve the Bateman equations and predict the time-dependent isotopic activity of the PuO_2 fuel based on the initial composition [14]. The Bateman equation, shown in Eq. (1), is solved in annual increments over a range of 100 years, and the time-dependent isotopic composition of the fuel is determined [15].

$$N_n(t) = \sum_{i=1}^{n}\left[N_i(0) \times \left(\prod_{j=1}^{n-1}\lambda_i\right) \times \left(\sum_{j=1}^{n}\left(\frac{e^{-\lambda_j t}}{\coprod_{p=i,p\neq j}^{n}(\lambda_p - \lambda_i)}\right)\right)\right] \quad (1)$$

The decay for isotopic sources of ^{236}Pu and ^{238}Pu, along with decay and production processes for all relevant subsequent elemental generations, can be found in Table 4 and is presented to illustrate the general decay and production trends of all elements involved in the decay chain. Given these time-dependent isotopic abundance data, the individual weights of each isotope at any given time-step can be calculated and assigned a fractional value of the total fuel mass.

Using this isotopic abundance weighting scheme, the individual gamma spectrum for each weighted isotope was then obtained from the National Nuclear Data Center (NNDC) databases [16]. These data allowed the inclusion of individual gamma line energies and intensities for each weighted isotope, which allowed for a weighted composite gamma spectrum to be created for any time-step requested. The gamma spectrum weighting method is shown in Equation (2).

$$F_i(t) = \frac{A_i(t)}{\sum_{j=1}^{n} A_j(t)} \quad (2)$$

Equation 2 shows where $F_i(t)$ represents the fraction of the total fuels' activity represented by an individual isotope (i) at a given time (t). Equation (3) shows the inclusion of the intensity (I_γ) of the specific gamma lines (of a specific isotope) and weights them to the isotopic abundance of an isotope (i).

$$I_{\gamma_{ij}} = F_i(t) I_{\gamma_j} \quad (3)$$

Finally, the composite spectrum for a fuel mass at a given time is compiled by combining all weighted gamma intensities ($I_{\gamma_{ij}}$) into a single spectrum. An example of a 10-year-old spectrum and its contributing isotopes can be seen in Figure 7. Once calculated, these composite gamma spectra are written into the MCNP6 input file as a discretized, energy-dependent gamma source term. These methods of determining time-dependent gamma activities and spectra were also performed using ORIGEN in SCALE 6.2 to further validate the aging effects calculated with IsoChain [17].

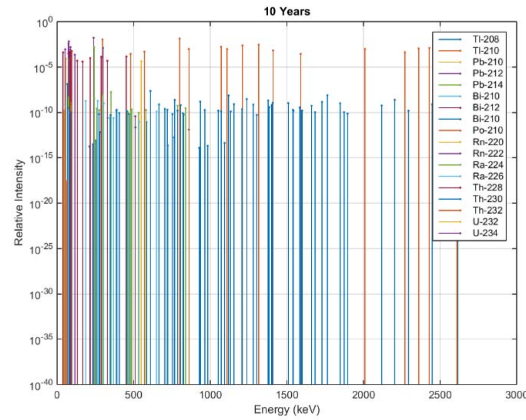

Figure 7. Example of composite gamma-ray spectrum for 10-year-old PuO_2 fuel.

Time-Dependent Neutron Spectra

Multiple channels of neutron production are present in PuO_2 fuels used for RPS technology. These channels represent spontaneous fission, as well as (α, n) reactions via interactions with low-Z impurities and ^{18}O isotopes in the surrounding RPS materials and PuO_2, fuel respectively [6]. Previous investigations of neutron radiation from PuO_2 fuel were performed by NASA's Jet Propulsion Laboratory (JPL), and the resulting neutron contributions for each channel are shown in Figure 8 [6].

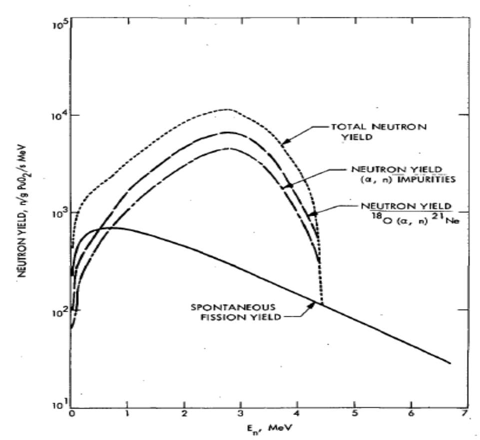

Figure 8. Neutron spectra based on spontaneous fission and various other (α, n) reactions.

Although these data (Figure 8) were originally used as a static neutron spectrum for all RPS-DET simulations, updates were made using the SCALE 6.2 ORIGEN depletion code to more accurately reflect the aging effects of the fuel over time. This is performed by allowing ORIGEN to solve the Bateman equations for the initial fuel's isotopic composition and to iteratively determine the specified 100-group neutron fluxes produced by spontaneous fissions and (α, n) reactions. These spectra are calculated for every year over the course of 100 year; Figure 9 shows a sample of these spectra to illustrate the general time-dependent neutron spectral changes within RPS-DET.

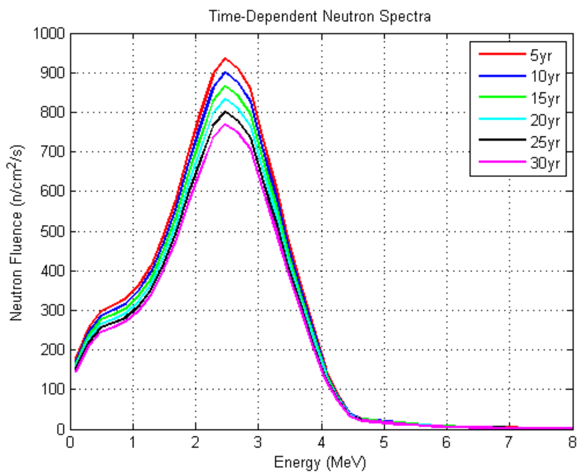

Figure 9. Example of how aging fuel affects neutron spectra over 30 years in RPS-DET.

The calculations performed in ORIGEN yielded a lower, beginning-of-life (BOL) neutron activity than measurements taken at Los Alamos National Laboratory (LANL) for a 2.2-kW Multi-Hundred Watt (MHW) fuel [18]. ORIGEN calculated (based on fuel composition assumptions) that the BOL-specific neutron activity is ~6,232 n/s/g-PuO_2, while LANL measured ~11,400 n/s/g-PuO_2. This discrepancy is likely due to compositional assumptions for light-Z materials (specifically ^{18}O) in the fuel causing a difference in (α, n) reactions which can dramatically alter the resulting neutron signature.

Tallies

RPS-DET currently uses two separate MCNP input decks for a single simulation—one for neutron source particles, and another for gammas. Initially, certain computational considerations drove the decision to separate the source terms, but future iterations of RPS-DET will most likely combine them into a single input deck. Regardless, each respective input deck currently tallies only neutrons or gammas and is performed by using what is referred to as a *mesh tally*. The mesh tally used in these simulations is a rectangular shape encompassing the entire geometry, spanning from ⁻500–+500cm along the X, Y and Z axes (about the origin) and divided into one million equally sized 10 cm^3 volumes. Each of these volumes tallies the fluence of the desired particle as it passes through it and provides the result in units of #/cm^2/src, where *src* is the number of source particles.

These particle fluence tallies are not combined yet, as they are species-specific and must first be normalized to the respective particle activity independently. This normalization is performed by using the time-dependent activities previously discussed and fitting them for ease of use. The gamma activity is outlined by the piecewise function shown in Eqs. (4 and 5), where time (t_{yr}) is in units of years. These functions were derived from a piecewise polynomial fit of the total gamma activities produced by the isotopes in Table 4.

<20 yr

$$A_{sp}(t_{yr}) = -5.602E3(t_{yr})^2 + 1.00E6(t_{yr}) - 3.56E3 \qquad (4)$$

≤ 20 yr

$$A_{sp}(t_{yr}) = -3.64E3(t_{yr})^2 + 1.00E6(t_{yr}) + 2.00E6 \qquad (5)$$

The neutron activity is also functionalized, and the resulting activity trend is shown in Eq. (6).

$$A_{sp}(t_{yr}) = 1.30E^{-}1(t_{yr})^2 +^{-}46.70(t_{yr}) + 6.23E3 \qquad (6)$$

The general time-dependent trends of the neutron and gamma activity are plotted together in Figure 10.

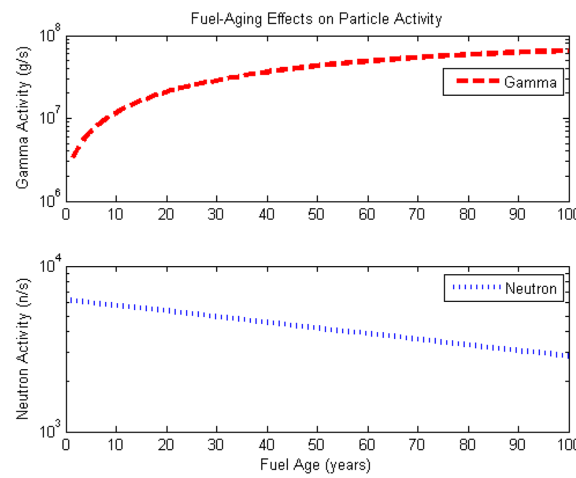

Figure 10. Particle activities for gammas (top) and neutrons (bottom) over a 100-year timeframe.

The absorbed dose and dose equivalent in tissue is calculated using fluence-to-dose conversion factors as outlined by the International Commission on Radiological Protection (ICRP) 116 for gammas and in further work by Veinot, et al., for neutrons [19,20]. These conversion factors were multiplicatively applied to the fluence tallies to convert MCNP units from #/cm^2/src to mGy/hr and mSv/hr. Further unit analysis was performed during post processing to produce units of mRAD/hr and mrem/hr, depending on the user's preference. It should be noted that all fluence-to-dose conversion factors used the anterior-posterior (AP) orientation.

The calculation of absorbed dose in silicon was performed in a manner similar to that used for dose in tissue except that fluence-to-dose conversion factors (FTDCFs) had to be developed specifically for silicon first. These FTDCFs were produced in MCNP6 by iteratively simulating a single volume of silicon, or a microchip, exposed to sequentially increasing mono-energetic neutrons and gammas, and then calculating the resulting absorbed dose inside the silicon-volume for each incident energy (Figure 11). The resulting FTDCFs were used as response functions in MCNP6 in the same way that the ICRP FTDCFs were used.

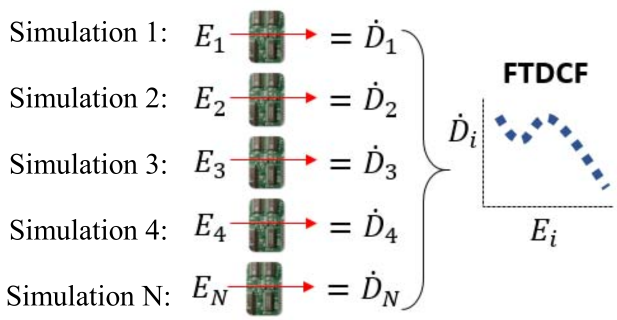

Figure 11. Illustration of FTDCF response function development.

3. Creation of Simulation Files

When RPS-DET is invoked for a simulation, it first creates a composite geometry based on the user-selected OOI and EOI. This is done by having the script read through the prewritten geometry libraries that are indexed according to a specific OOI or EOI number. Every OOI in the library is written to be bounded by a specific, commonly numbered surface (i.e., everything inside surface #100), and every EOI in the library is defined as everything outside the same specific numbered surface (i.e., everything outside surface #100). If the numbering scheme inside the RPS-DET libraries is maintained, any composite geometry made of OOIs and EOIs can be incorporated into the program and seamlessly combined into a composite geometry.

The source term is different for neutrons and photons, so each respective energy spectrum must be read in and then written out to the new input deck. The gamma and neutron spectra are referenced based on the user-selected fuel age. The spectra libraries consist of 100 separate text files, each representing a discrete, annual, energy-dependent source spectrum based on the isotopes previously discussed in Table 4.

The tallies are standardized in size, so they are written out the same for any composite geometry, source particle, and fuel age. A list of all mesh tallies included for every RPS-DET simulation can be seen in Table 5.

Although this section explains how construction of the MCNP input deck is performed, this process is automatically completed for the user based on the chosen OOI, EOI, and fuel age.

Table 5. Particle Tallies and Units Used in RPS-DET Simulations

Particle	Tally Description	Units after Conversion	Number of Tallies
Neutrons	Fluence	$\frac{n}{s \cdot cm^2}$	1
	Absorbed dose in tissue	mGy/hr & mRAD/hr	1
	Dose equivalent in tissue	mSv/hr & mrem/hr	1
	Absorbed dose in Silicon	Rad(Si)/hr	1
Gammas	Fluence	$\frac{n}{s \cdot cm^2}$	1
	Absorbed dose in tissue	mGy/hr & mRAD/hr	1
	Dose equivalent in tissue	mSv/hr & mrem/hr	1
	Absorbed dose in Silicon	Rad(Si)/hr	1
Total number of tallies per simulation:			8

4. Post Processing

When a given MCNP6 simulation is complete, two ~100Mb files (gammas and neutrons) are generated by MCNP, each containing the eight one-million-element mesh tallies. Upon completion of this process, the data can be loaded into the RPS-DET post-processing graphical user interface (GUI), where they may be visually investigated and saved as Matlab matrices (.m files). The image of the GUI in Figure 12 shows the visual presentation to the user, while Table 6 provides an explanation of each feature called-out in the GUI.

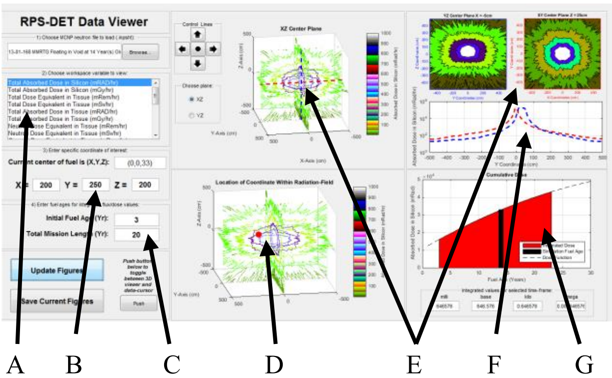

Figure 12. RPS-DET post-processing GUI features

Table 6. Explanation of Features in RPS-DET GUI

Feature	Brief Explanation
A	User selects data/units to be displayed: total, neutron or gamma, flux, dose equivalent in tissue, or absorbed dose in silicon or tissue
B	User enters specific XYZ coordinate of interest
C	User specifies initial age of fuel and duration of mission
D	3D display of flux/dose field with specific coordinate shown (in red)
E	Interactive 3D sliced planes (left arrow) and 2D contour maps (right arrow); 2D contour maps automatically update as 3D planes are manipulated
F	Centerline flux/dose profiles from interactive 3D planes which automatically update as 3D planes are manipulated
G	Estimated integrated flux/dose at user-specified coordinate (B) along with initial fuel age and mission length (C)

The features described in Table 6 show the ability of RPS-DET to present the spatial flux/dose fields around a given OOI, EOI, fuel-age configuration combination. It also allows a user to easily switch between SI and English units for any selection of neutron of gamma flux. Users can also look at combined absorbed and equivalent doses in multiple materials, as well as the neutron or gamma contribution to a specific total dose.

The integrated dose estimation for an individual coordinate can be used to identify cumulative irradiation implications for a given location that might be occupied by a person, electronic device or another material of interest. Having the ability to easily move this coordinate of interest in the 3D flux/dose field and see the various cumulative effects of the location-choice shortens the time required for lengthy calculations and can provide useful information when decisions are made regarding higher or lower consequence regions where radiation is of concern.

The method for estimating the cumulative dose presented in the GUI is shown as feature "G" in Figure 12. The method for calculating the integrated dose—$\int(D)dt$—for different OOIs in different EOIs has been simplified by the following process. First, OOIs were classified either as *shielded* or *not shielded.* For example, a single or multiple fueled clad or a single or multiple GPHS is considered an *unshielded* OOI, while any RPS system or full generator design is considered a *shielded* OOI (MMRTG, GPHS-RTG, ASRG, etc.). Whether shielded or not, the OOI is then simulated, floating in a void, at sequential time-steps of one year, from 0–30 years of age. Ten random coordinates are chosen within a radial band of >50cm and <300cm from origin to avoid either sampling inside the RPS or sampling in low statistics regions, respectively. These points are used as the same sampling positions at each year, for thirty years of time-dependent simulations (P1-P10 in Figure 13 and Figure 14 A and B).

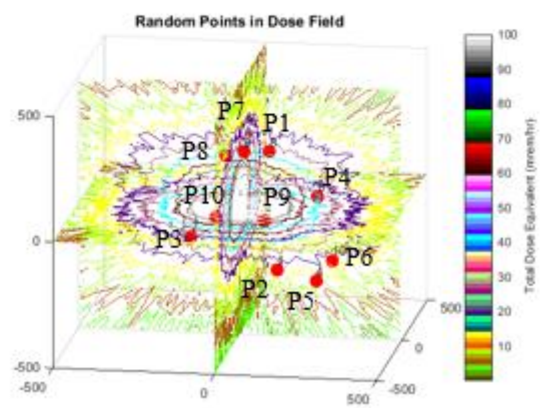

Figure 13. Example of 10 random sampling locations within flux/dose field.

For each OOI, the value corresponding to each coordinate (P1-P10) is represented as a function of fuel-age (Figure 14, A) and normalized to unit area and averaged between all ten trends (Figure 14, B). The resulting average is fitted with a second order polynomial, or aging function, which is used to project (forward or backward) in time, the expected dose trend of the neutron, gamma and combined flux/dose by means of interpolating and integrating the aging function between any time boundaries of interest from 0–30 years.

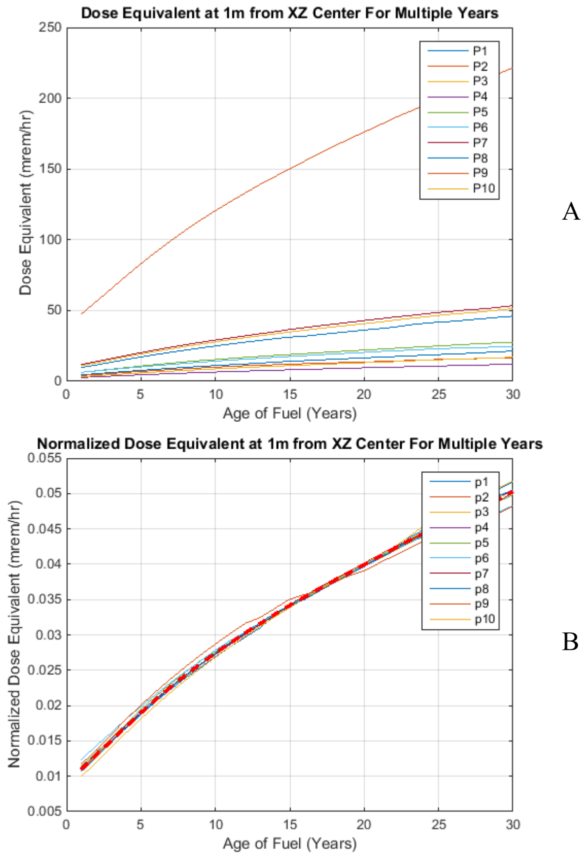

Figure 14. Flux/dose trends of ten random sample-points from 0–30 years (A); and normalized and averaged (red dashed line) trends from A used to fit a second order polynomial (B).

Once the normalized aging function—($D_{norm}(t)$—is calculated for the neutron and gamma-dependent values (flux/dose), a single scalar can be used to scale the entire function accordingly by multiplying it against the aging function. When a user selects a coordinate for inspection in the XYZ fields of the GUI, RPS-DET finds the corresponding flux/dose value at this location of interest, (D_{XYZ}), and this value corresponds to a specific fuel-age from the simulation. This value, D_{XYZ}, is then used as a target or ceiling when scaling the aging function by iteratively multiplying increasing scalars (S_i) against the aging function until $S_i D_{norm}(t) \approx D_{XYZ}$ (Figure 15).

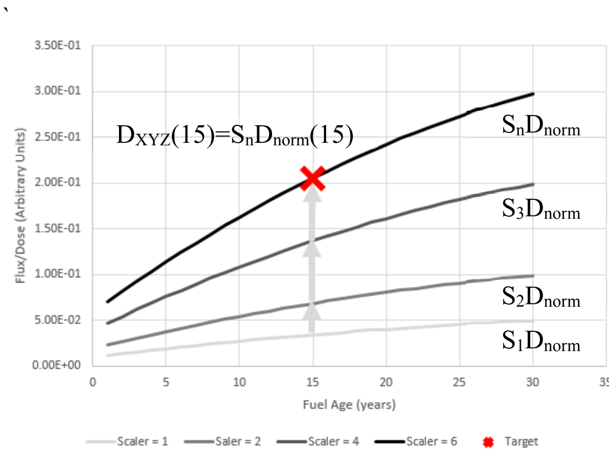

Figure 15. Example illustration of iteratively scaling the aging function (SnDnorm) until target value (DXYZ) is reached (fuel is 15 years old in this example).

This scaling approach of an averaged aging function exploits the observation that the aging trends for fuels are similar, for a similarly shielded OOI, and for all points within a given flux/dose field. The only difference between the values at different coordinates over time is a scaling factor. Matching an aging function in magnitude to the appropriate element of the aging function fixes the 30-year behavior of the value, allowing integration over time for a given coordinate and unit based on the value from a single simulation.

5. Benchmark Results

Specific benchmarks were chosen to compare the performance of RPS-DET. These benchmarks include measurements of the MMRTG used for the Mars Science Laboratory Curiosity (MSL) rover and the GPHS-RTG used for the New Horizons mission [11, 21]. These RPS units were measured at multiple sites by multiple agencies under varying circumstances. Comparisons of data for these two benchmarks are included in this section.

Due to the limited availability of detailed information regarding the average age of the fuel contained in a measured RTG and the potential differences caused by unknown compositions of (α, n)-inducing materials, assumptions were made for each benchmark simulation based on educated guesses for fuel age and fuel composition. All RPS-DET simulations derive results from 10x10x10cm tallying volume with the value of this volume reported at its geometric center. For this reason, a ±5 cm uncertainty bound is reported for all distances pertaining to RPS-DET results.

MMRTG

The MMRTG used on the MSL was loaded with 8 GPHSs at INL prior to shipment to Cape Canaveral in 2011 [22]. This MMRTG was assessed by NASA Jet Propulsion Laboratory

(JPL) staff during systematic flight testing and again by INL staff during assembly and prior to transportation [22]. Biological dose rate measurements were acquired and used in this work as a benchmarking metric for biological dose equivalent predictions using RPS-DET [22]. No comparative measurements determining the absorbed dose in silicon from an MMRTG have been obtained at this point, but at this writing, it is assumed that if RPS-DET predictions of biological dose equivalent are relatively accurate when compared to field measurements, then predictions for absorbed dose in silicon may be relatively accurate, as well. Comparisons of RPS-DET dose rate predictions with measurements can be seen in Figure 16.

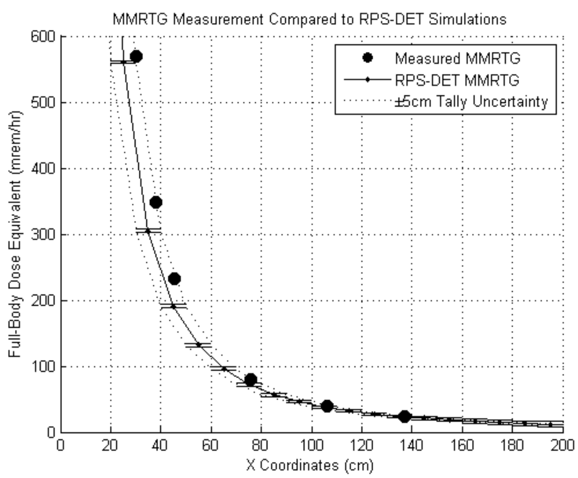

Figure 16. Comparison of results from RPS-DET simulation of MMRTG to field measurements.

RPS-DET assumes 3-year-old fuel for the MSL-MMRTG simulation, suspended in air. The MMRTG measurements are within, at most, ~5% of RPS-DET simulation uncertainties.

GPHS-RTG

The source of this measurement came from INL's occupational dose measurements for the F8 GPHS-RTG for the Pluto New Horizons in 2005 (Figure 17) [22]. The GPHS-RTG contains 18 GPHSs and RPS-DET assumed an average 10-year-old fuel for this simulation to account for a portion of the fuel in this mission being ~20-years-old [23].

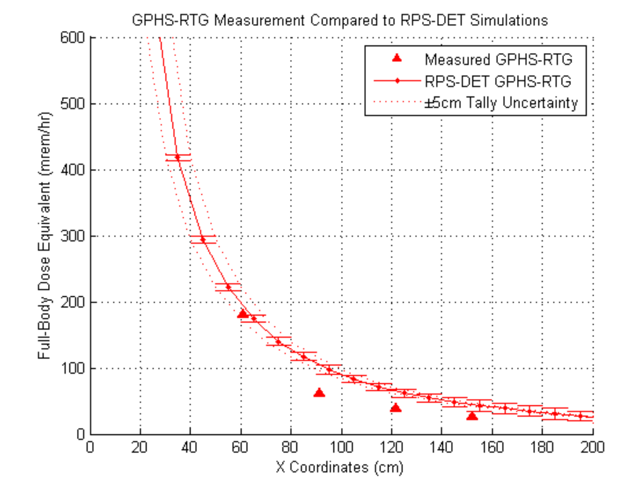

Figure 17. Comparison of results from RPS-DET simulation of GPHS-RTG to field-measurements.

The dose rate prediction made by RPS-DET for the New Horizon GPHS-RTG are within, at most, 50% of measured values around 90 cm from centerline. Disagreements may be due to a difference between the actual fuel composition and age and the simulation assumptions for these variables. Uncertainties in the measured values from both MMRTG and GPHS-RTG were not available for these comparisons, which may also exaggerate some discrepancies.

6. EXAMPLES OF RPS-DET APPLICATIONS

Limitless combinations and comparisons could be analyzed with RPS-DET or a similar tool; a few relevant examples are presented below. While the following examples are valid, they are presented here to show some of the capabilities of RPS-DET and should not be considered definitive results. Future publications and/or analyses using RPS-DET as a tool for specific comparative investigations may follow, while less detail will be focused on the development of RPS-DET and more on the analysis at hand.

The following results will be presented in a consistent format with the axis-orientation for a given OOI shown in Figure 18. The marker on the x-axis of Figure 18 is an arbitrary coordinate that is typically 1m along the x-axis, and it is used as a comparative metric between different simulations. Figure 19 (left) is the flux/dose value along the x-axis of each simulation, and the red dashed line corresponds to the comparative marker example on the x-axis of Figure 18. Data similar to the bar graph in Figure 19 (right) will be used to show specific values at the comparative coordinate to better highlight any relationships between the compared simulations.

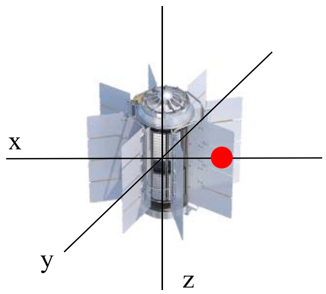

Figure 18. Axis orientation for all results shown in this section. The red marker corresponds to some arbitrary coordinate along the x-axis used for comparative purposes in the following figures.

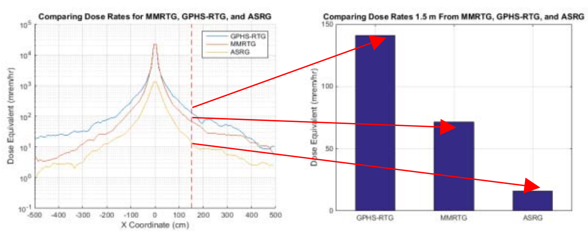

Figure 19. Flux/dose projection along X-centerline axis; the red dashed line corresponds to a location along the x-axis in Figure 18 (left); bar graph illustrating relationship of values at the coordinate of comparison represented by the red dashed line (right).

Comparing Static and Dynamic RPS Designs

Since the objective for developing RPS-DET was focused on analyzing the radiation implications of new dynamic RPS systems, an obvious application of interest for this tool is to inter-compare existing RPS systems alongside proposed dynamic systems in the same environment with the same aged fuel. Figure 20 shows a comparison of the MMRTG, GPHS-RTG, and the Advanced Stirling Radioisotope Generator (ASRG) design all floating in a void with 10-year-old fuel.

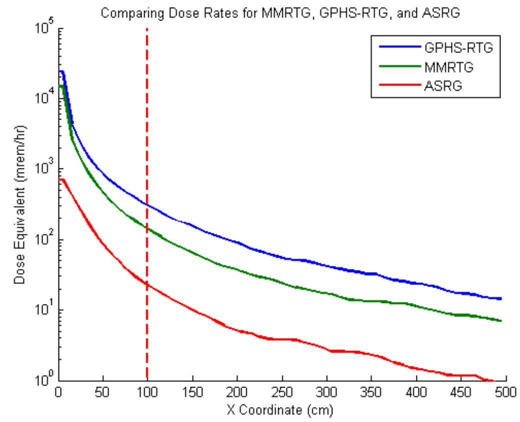

Figure 20. Comparing X-centerline dose rates for MMRTG, GPHS-RTG and ASRG. Dose rates intersecting the red dashed line at 1.0 m are displayed in Figure 21.

Given that the GPHS-RTG (blue line) has 18 GPHSs, it is not surprising that the radial dose rate trend in Figure 20 is generally higher than the MMRTG (green line), which contains only 8 GPHSs. The ASRG model consists of only 2 GPHSs which are physically separated from one another by tens of centimeters by various Stirling engine components [24]. Conversely, the MMRTG and GPHS-RTG both have vertically stacked GPHS configurations, which noticeably increase the particle flux inside and outside the RPS housing over a given area when compared to the ASRG's lower density radiation profile. Figure 21 shows the dose rate at 1.0 m off centerline along the x-axis between the three RPS models, highlighting the general trend of the dose profiles for a fixed coordinate.

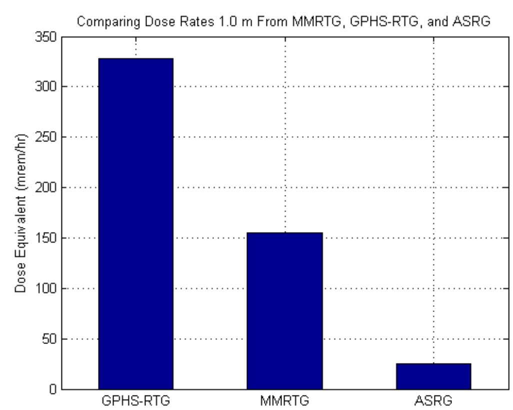

Figure 21. Comparing the dose 1.0 m from centerline (red dashed line in Figure 20) along the X-axis between a GPHS-RTG, MMRTG and an ASRG.

Comparisons between differing RPS designs serve as a motivator for the development of RPS-DET, and instructive results may be obtained from comparisons of this nature. As new RPS models are proposed/designed, they can easily be written into the RPS-DET library, inter-compared against existing models, and then comparative conclusions can be drawn.

Dose Rate Effects from GPHS Vertical Stacking Schemes

Although the examples in Figure 20 and Figure 21 show the difference in dose fields between RPS systems, other fundamental aspects for RPS design are also of interest. Because the vertical stacking of GPHSs for traditional RTG units is common practice and certain dynamic conversion systems may use stacking designs too, RPS-DET can illustrate some quantitative perspectives on dose implications as a function of GPHS number by showing sequentially stacked GPHSs and illustrating how this affects the ambient dose field. Figure 22 shows x-centerline dose rate profiles for progressively stacked GPHSs, while Figure 23 shows the dose rate for each GPHS configuration at a constant radial distance of 1.0 meter from x-centerline.

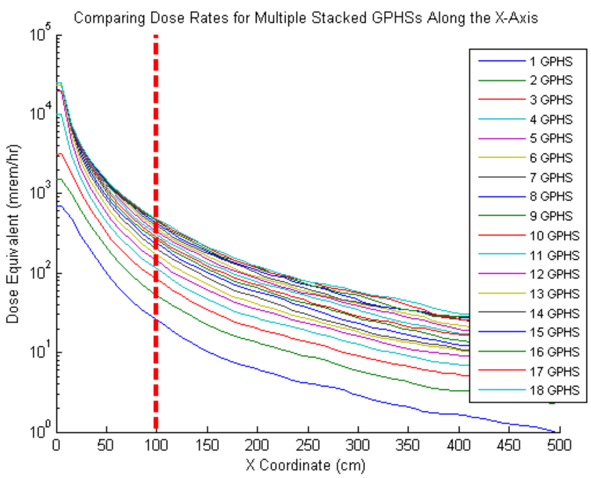

Figure 22. Comparing x-centerline dose rates for 1–8 GPHSs stacked vertically, floating in air; dose rates intersecting the red dashed line at 1.0m are displayed in Figure 21.

Figure 23 shows that there is a linear increase in dose rate as a function of the GPHS number if they are vertically stacked. As future models of some DRPS systems may incorporate traditional RTG stacking methods, it would be valuable to rapidly asses the radiation impacts to the ambient environment as a function of the GPHS number. Although this linear trend of dose, as a function of the GPHS number, may be present for flux/dose values perpendicular to a GPHS-stack's vertical axis, this trend is not necessarily true above and below the top and bottom GPHSs in a given stack.

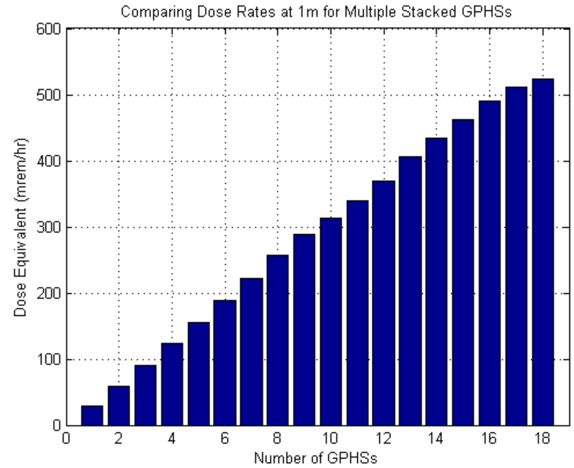

Figure 23. Comparing the dose at 1.0 m from centerline (red dashed line in Figure 22) along the X-axis for sequentially stacking 1–18 GPHSs.

Effects of Aging Fuel in Single RPS Design

Given the effects discussed previously regarding the increase over time of higher energy gamma-rays with the production of daughter isotopes like bismuth, thallium, and lead, capturing the average age or blend of a given RPS fuel is of great importance in predicting the ambient radiation field. By the isotopic decay and production processes within PuO_2 fuel, there is naturally a more-significant increase of activity, and thus dose, within the first 20–25 years following production. Figure 24 shows the effects of the x-centerline dose profiles of an MMRTG as a function of fuel age. The dashed red line marks a 1.0m distance used for comparative purposes in Figure 25 and highlights the specific dose-rates for each fuel age.

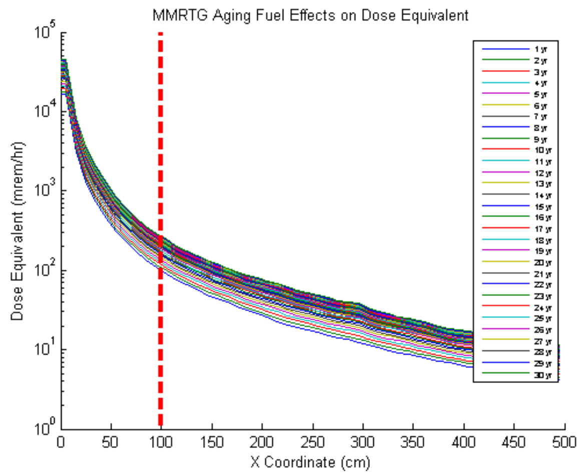

Figure 24. Comparing x-centerline dose rates for 1–100-year-old PuO_2 fuel in 25-year increments (dose rates intersecting the red dashed line at 1.0 m are displayed in Figure 25).

This fuel aging relationship is important to understand given that an RPS system will typically have the highest biological dose concerns during terrestrial fabrication, and at least for unmanned missions, there will be no interest or concern for biological dose once the system has been launched. Furthermore, for cumulative electronic dose over the life of a mission, it is important to understand dose trends over large lengths of time to accurately represent the true implications of aging fuel and how it affects the radiation fields in and around RPS systems.

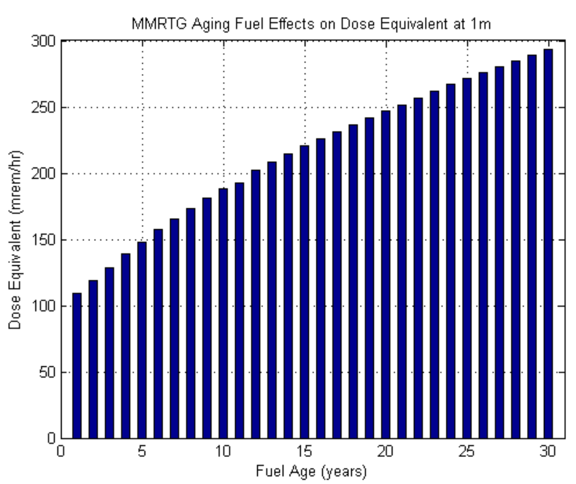

Figure 25. Comparing the dose rate at 1.0 m along x-centerline (red dashed line in Figure 24) for 1–30-year-old PuO_2 fuel.

Effects of Placing a Single RPS in Varying Environments

The ambient flux/dose field is altered by the surrounding environment through methods such as, but not limited to, atmospheric attenuation of radiation and reflected neutrons causing elevated flux/dose profiles in confined spaces. Being able to represent multiple environmental scenarios for a single RPS is of value for calculating accurate cumulative radiation estimates.

For example, to address the effects of the surrounding environment, an MMRTG with 10-year-old fuel is simulated at sea level (air) on Earth while inside a concrete room, then in a generic spacecraft aeroshell, and then on the Martian surface. The dose trends of these three scenarios are compared in Figure 26 and Figure 27.

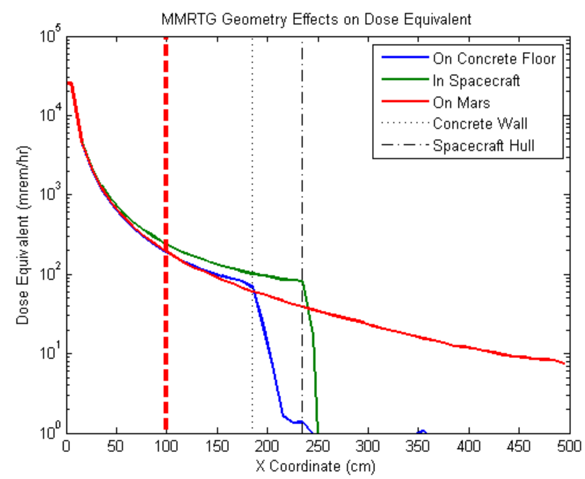

Figure 26. Comparison of an MMRTG with 10-year-old fuel in three separate environments (black vertical dashed lines mark geometric boundaries for relevant environmental features; red dashed line represents sampling coordinate at 1.0 m displayed in Figure 27.

Figure 26 and Figure 27 show that different environmental scenarios can have significant effects on the radiation field for a same-aged RPS unit. The dose inside the capsule is higher than the dose on the concrete floor on Earth. This is largely due to the confinement and reflection of neutrons in the ambient dose field and the lack of an atmosphere. Furthermore, the dose on the Martian surface is slightly higher (~2% increase) than the Earth-based simulation (~208 mrem/hr vs ~204 mrem/hr) due to the significant differences in atmospheric pressure for each environment as a result of the differing ambient densities of each atmosphere. Although this specific dose comparison is not a significant difference between the Earth-to-Mars atmospheres in dose rates, a difference of 4 mrem/hr over a single decade can accumulate to hundreds of Rem or RAD, which should not be neglected in simulation predictions.

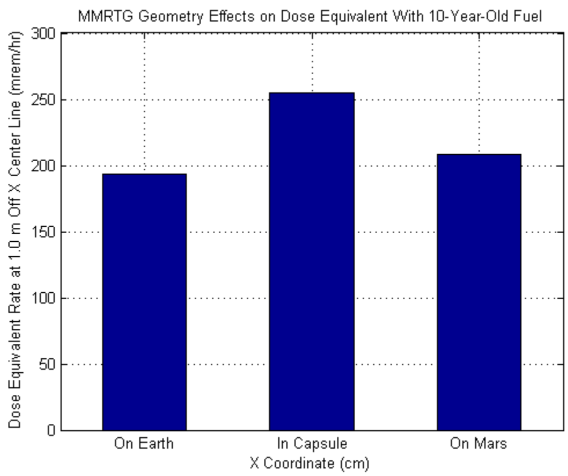

Figure 27. Dose values at 1.0 m along x-centerline (red dashed line in Figure 26).

Calculating Cumulative Dose for Complex Mission Lifetimes

Although it is important to accurately assess the impacts of environmental scenarios on the radiation field of a given RPS, it is crucial to also consider the effects of fuel aging for a more accurate estimate of a complex mission lifetime. RPS-DET allows an analyst to build a series of expected environments, place the OOI in each environment for a given duration, project the integrated dose profile for that given duration, change to a new environment with a new aged fuel, and repeat the process to determine a more accurate estimate of the total cumulative dose from a complex mission profile.

For example, in the previous illustration (Figure 26 and Figure 27), an MMRTG with 10-year-old fuel was placed in three separate environments, and no integrated dose profiles were projected. Although this type of comparison may be of importance for determining environmental effects, it is insufficient for determining true dose implications because it does not represent the aging effects of the fuel for a true mission profile. In this example, the same MMRTG is placed in the same three environments, but the fuel will be aged according to a speculative mission profile. The MMRTG will now be in the Earth environment for 5 years (ages 0–5 years), the spacecraft for 1 year (ages 5–6 years), and on the Martian surface for 12 years (ages 6–18 years). The projected aging functions of the respective environments will be used to demonstrate the ability to project an integrated dose as a function of both fuel age and environmental surroundings. Figure 28 shows the new dose profiles for the three scenarios, while Figure 29 shows the comparison of the original 10-year-old MMRTG fuel alongside the new, appropriately aged fuel at a 1.0m distance along the x-axis.

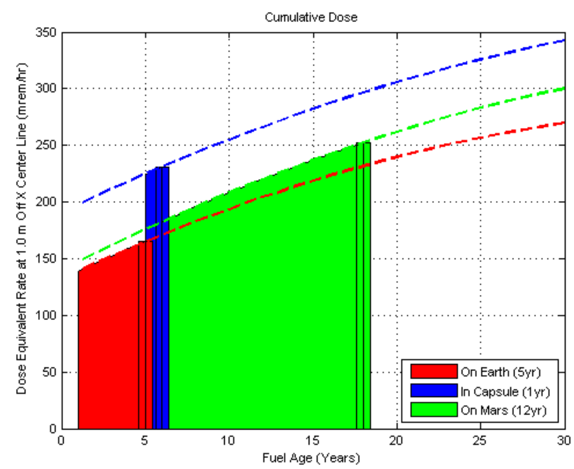

Figure 28. Projected and integrated doses for complex mission lifetime.

Figure 28 shows the importance of reflecting the age, OOI, and EOI when performing a cumulative dose prediction for a given series of mission environments by highlighting the differences in magnitude and the projected aging function of each individual scenario. This method of calculating integrated doses over a complex mission lifetime allows accurate predictions of ambient radiation effects by reflecting environmental effects along with changes in fuel-radiation characteristics.

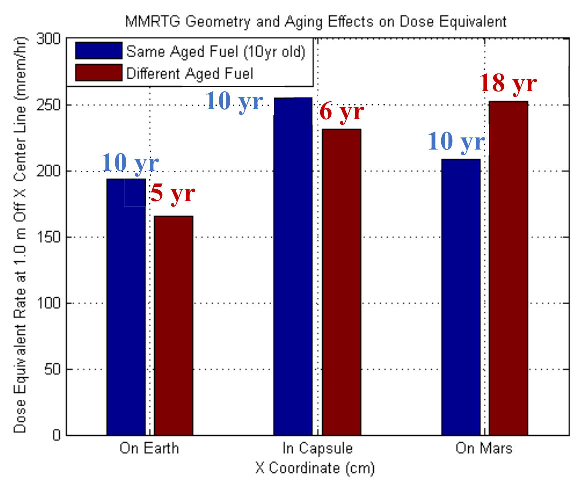

Figure 29. Comparison of the same OOI in different EOIs for a fuel age of 10 years (blue) and of different fuel ages (red).

Finally, examples of observing the effects of environmental conditions on radiation fields are qualitative and quantitative ways to illustrate and explore simulation results. Figure 30 (A–F) shows a 10-year-old MMRTG in various EOIs and illustrates how that surrounding environment alters the ambient radiation field.

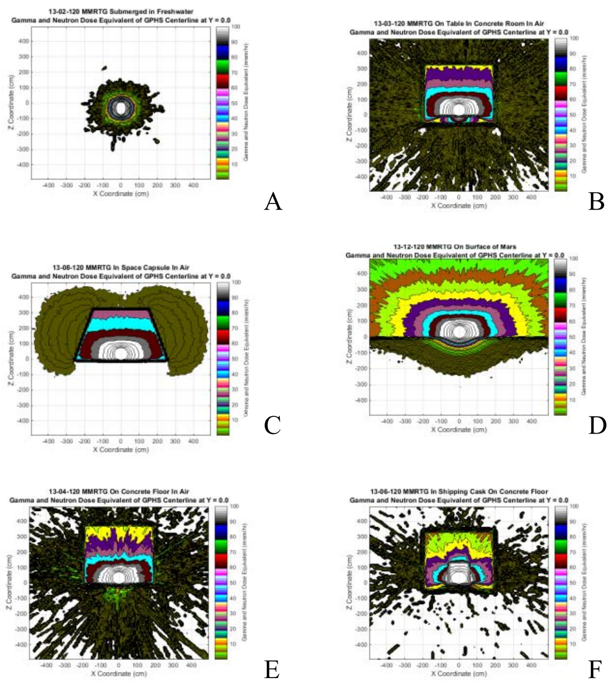

Figure 30. RPS-DET examples of radiation field from 10-year-old fuel in an MMRTG under water (A), on a table in a concrete room (B), in a generic spacecraft (C), on the Martian surface (D), on the floor of a concrete room (E), and in a #9904 shipping container (F).

Figure 30 shows a few examples of EOI-effects on a given RPS, which are used here to demonstrate more comparative features of the RPS-DET tool. A user can interactively inspect any flux/dose map (similar to Figure 30) produced by RPS-DET to deduce the qualitative effect of the greater radiation field and the exact value of the flux/dose at any location in the simulation space.

7. Future Work

Investigations will continue to determine whether discrepancies between RPS-DET and measurements are due to measurement-related uncertainties or incongruent assumptions in the simulation process. Dose equivalent has been the chosen comparative metric for benchmarking thus far, as these are the only well-documented measurement values that have been available for comparison. Future benchmarking efforts will acquire and investigate more field measurements, along with other independent simulations.

Future iterations of RPS-DET will incorporate more RPS models and relevant environments as they become available for inclusion in the OOI and EOI libraries.

RPS-DET plans to incorporate a means to combine the total fuel composition as a function of individual pellet-age to gain a better representation of the total or average RPS fuel age. Having more accurate control over these parameters will aid in producing more accurate predictions for the mission lifetime of a given RPS unit, and it will allow for more relevant comparisons between RPS-DET simulations and benchmarking values.

As there are many sources of ambient radiation imparted to an electronics system through the lifetime of a mission, and as RPS-DET currently only provides the contribution produced by RPS fuel sources, it is of interest to include a feature in RPS-DET that calculates and simulates incurred dose from galactic cosmic rays, solar winds, and charged particle belts of celestial bodies such as Earth, Jupiter, and Saturn based on duration, solar cycle, flyby trajectories, and other relevant mission parameters. This effort would not be trivial, but it may be prudent for future analyses of mission-critical electronic components while undertaking a radiation modeling approach to RPS systems and ambient radiation fields for spacecraft with RPS-DET.

8. Conclusions

The purpose of RPS-DET is to develop a rapid dose estimation tool for estimating the dose implications of new DRPS systems being evaluated by the DOE and NASA.

Because no dynamic DRPS systems have achieved flight status and thus have not been fully loaded with real PuO_2 fuel for significant durations, past RTG models have been used to benchmark the performance of RPS-DET. As future DRPS units are developed, vetted, and tested, RPS-DET can serve as a portion of the greater mission analysis by accurately and efficiently predicting the biological dose equivalent concerns during fabrication, assembly, and installation here on Earth, along with the cumulative dose incurred by nearby electronics over an entire mission lifetime. RPS-DET has shown the ability to provide dose estimations in multiple environments of interest while using multiple RPS models and fuel configurations of interest. Furthermore, the ability to capture the changes in gamma and neutron emission as a function of time allows much flexibility in providing dose estimations specifically during the first ~30 years of fuel life.

RPS-DET is currently a functioning tool which represents complex simulation environments, allowing an analyst the ability to rapidly deduce cumulative flux/dose caused by a specific RPS unit for humans and electronics through an entire mission lifetime. This ability will aid investigators in efficiently and accurately deducing the radiation implications of new DRPS units as they are proposed and evaluated in preparation for flight. It will also provide the ability to analyze traditional RTG designs still being used for space missions. Whether the source of radiation is a dynamic or static RPS, RPS-DET serves to estimate the radiation implications to humans, electronics, and materials during assembly and over entire complex mission lifetimes.

Acknowledgments

This manuscript has been authored by UT-Battelle, LLC, under contract DE-AC05-00OR22725 with the US Department of Energy (DOE). The US government retains and the publisher, by accepting the article for publication, acknowledges that the US government retains a nonexclusive, paid-up, irrevocable, worldwide license to publish or reproduce the published form of this manuscript, or allow others to do so, for US government purposes. DOE will provide public access to these results of federally sponsored research in accordance with the DOE Public Access Plan (http://energy.gov/downloads/doe-public-access-plan).

This work was funded by the NASA RPS Program Office, and much appreciation is given to them and Glenn Research Center for their guidance and support, specifically June Zakrajsek and Paul Schmitz. Field measurements, fueling details, and detailed information regarding MMRTG and GPHS-RTG were provided by Dr. Steve Johnson and Kelley Lively at INL. Information regarding the materials and dimensions of MMRTG were provided by Bill Otting of Aerojet Rocketdyne. This work was initiated while the author was attending the University of Tennessee, and many technical contributions were made by Dr. Lawrence Heilbronn from the Nuclear Engineering Department. Special thanks to Dr. Lou Qualls at Oak Ridge National Laboratory (ORNL) for his mentorship and instruction during this project.

References

[1] R. L. Cataldo and G. L. Bennett, “US Space Radioisotope Power Systems and Applications: Past, Present and Future,” NASA Jet Propulsion Laboratory (JPL), JPL Publication 15–6, 2011.

[2] NASA, “Research Opportunities in Space and Earth Sciences - 2016.” [Online]. Available: https://nspires.nasaprs.com/external/viewrepositorydocument/cmdocumentid=498219/solicitationId=%7B6352B2ED-E22A-20BB-129D-BD0993BE2AD8%7D/viewSolicitationDocument=1/FULL%20ROSES%202016_amend58.pdf. [Accessed: 25-Sep-2017].

[3] A. Campbell, P. McDonald, and K. Ray, “Single event upset rates in space,” *Nucl. Sci. IEEE Trans. On*, vol. 39, no. 6, pp. 1828–1835, 1992.

[4] R. Manning and W. L. Simon, *Mars rover Curiosity : an inside account from Curiosity’s chief engineer*. Washington, DC: Smithsonian Books, 2014.

[5] R. Kruse, “Historic Spacecraft.” [Online]. Available: http://historicspacecraft.com/Probes_Mars.html. [Accessed: 01-Jan-2016].

[6] M. Taherzadeh, “Neutron Radiation Characteristics of Plutonium Dioxide Fuel,” JPL, Pasadena, CA, 32–1555, 1972.

[7] T. Goorley *et al.*, “Features of MCNP6,” *Ann. Nucl. Energy*, vol. 87, pp. 772–783, 2016.

[8] J. Grandidier, J. Gilbert, and G. Carr, “Cassini Power Subsytem,” presented at the Nuclear & Emerging Technologies for Space (NETS), Orlando, FL, 2017, pp. 74–81.

[9] R. Bechtel, “Multi-Mission Radioisotope Thermoelectric Generator (MMRTG).” [Online]. Available: https://www.nasa.gov/sites/default/files/files/4_Mars_2020_MMRTG.pdf. [Accessed: 15-Sep-2016].

[10] T. G. George and D. Pavone, *General-purpose heat source safety verification test series: SVT-11 through SVT-13*. Los Alamos National Laboratory, 1986.

[11] H. International, “Haynes 25 Alloy Online Product Brochure.”

[12] T. Ceramics, “Min-K Data Sheet,” 1999. [Online]. Available: http://inproheat.com/sites/files/documents/Min-K_%20Moldable.pdf.

[13] J. C. McCoy, “An Overview of the Radioisotope Thermoelectric Generator Transportation System Program,” Westinghouse Hanford Company, 1995.

[14] C. L. Almanza, H. A. Lovett, F. Schmitrroth, M. A. Garland, and S. Mirzadeh, “Iso-Chain: A User Friendly Two-Group Nuclear Transmutation and Decay Code,” presented at the ANS Mid-Winter 6 Meeting and Technology Expo, 2006, pp. 441–442.

[15] H. Bateman, “Solution of a System of Differential Equations Occurring in the Theory of Radioactive Transformations,” *Proc. Camb. Philos. Soc. Math. Phys. Sci.*, vol. 15, 1910.

[16] “National Nuclear Data Center Interactive Chart of Nuclides.” [Online]. Available: http://www.nndc.bnl.gov/chart/. [Accessed: 01-Jan-2016].

[17] W. Wieselquist, “Capabilities of ORIGEN in SCALE 6.2,” 19-Jul-2016.

[18] G. M. Matlack and C. F. Metz, “Radiation Characteristics of Plutonium-238,” Los Alamos National Laboratory, Los Alamos, NM, LA-3696, 1967.

[19] K. Eckerman, J. Harrison, H. G. Menzel, C. H. Clement, and others, “ICRP publication 119: compendium of dose coefficients based on ICRP publication 60,” *Ann. ICRP*, vol. 42, no. 4, pp. e1–e130, 2013.

[20] K. G. Veinot and N. E. Hertel, “Effective quality factors for neutrons based on the revised ICRPICRU recommendations,” *Radiat. Prot. Dosimetry*, vol. 115, no. 1–4, pp. 536–541, 2005.

[21] G. L. Bennett *et al.*, “Mission of daring: the general-purpose heat source radioisotope thermoelectric generator,” in *4th International Energy Conversion Engineering Conference and Exhibit (IECEC), San Diego, California, AIAA*, 2006, vol. 4096, p. 2006.

[22] "Electronic communication (email) with Director of Space and Nuclear Power and Isotope Technologies Division at Idaho National Laboratory," 08-Mar-2017.
[23] B. Bairstow and Y. Lee, "Radioisotope Power Systems Reference Book for Mission Designers and Planners," 2015.
[24] N. A. and S. Administration, "Advanced Stirling Radioisotope Generator (ASRG) Fact Sheet," NF-2013-07-568-HQ, 2013.

BIOGRAPHY

Michael B. R. Smith *received a BS in Nuclear Engineering with a concentration in Radiological Nuclear Engineering from The University of Tennessee (UTK) in 2016. He went on to earn his MS of Science from the Department of Nuclear Engineering at UTK in 2017. He has been involved in internships and research projects throughout this time covering topics such as nuclear thermal propulsion, galactic cosmic ray transport, radioisotope power sources, and prompt neutron background signals at the Spallation Neutron Source. He has worked in a post-master's position at ORNL since his graduation supporting the Advanced Reactor and Safety Systems team. Michael is currently serving as a consultant on multiple NASA-funded projects involving radioisotope power source technologies, including dynamic radioisotope power source technology assessments and the Mars 2020 MMRTG surrogate mission team. Prior to his work in nuclear/space sciences, he worked in the maritime industry for over 10 years as a manned submersible pilot, boat captain, and commercial diver.*